African Journal of Biotechnology Vol. 10(60), pp. 13004-13013, 5 October, 2011
Available online at http://www.academicjournals.org/AJB
DOI: 10.5897/AJB10.1727
ISSN 1684–5315 © 2011 Academic Journals

Full Length Research Paper

Proteomic analysis of human oral verrucous carcinoma

Yuehong Wang[1], Zhangui Tang[1,2]*, Suping Zhao[3], Xiaoli Xie[1], Zhigang Yao[4], Chenghui Liu[1], Binbin Qu[1], Yan Chen[5], Zhixiang Xiao[5] and Guiyuan Li[2]

[1]Department of Oral and Maxillofacial Surgery, Xiangya Hospital and School of Stomatology, Central South University, Changsha 410078, China.
[2] Institute of Oncology, Central South University, Changsha 410078, China.
[3]Department of Otolaryngology and Head & Neck Surgery, Xiangya Hospital, Central South University, Changsha 410078, China.
[4]Department of Oral Histology and Pathology, Xiangya Hospital and School of Stomatology, Central South University, Changsha 410078, China.
[5]Key Laboratory of Cancer Proteomics of Chinese Ministry of Health, Changsha 410008, China.

Accepted 20 June, 2011

This study is about proteomic analysis of oral verrucous carcinoma (OVC). The total proteins obtained from tumour and adjacent normal oral mucosa of patients with OVC and oral squamous cell carcinoma (OSCC) were separated with two dimensional electrophoresis (2-DE) by using immobilized pH gradient strips and visualized by staining with silver nitrate. The gel images were acquired by scanner and 2-DE analysed by image master 2D elite. Twenty distinct protein spots were excised from gel randomly and digested in gel by TPCK-trypsin. Mass analysis of the tryptic digested peptides mixture was performed by using MALDI-TOF-MS. Peptide mass fingerprints (PMFs) obtained by the MALDI-TOF analysis were applied to National Center for Biotechnology Information (NCBI), SWISS-PROT and MSDB databases using Mascot software. Then the 2-DE gel imaging showed that 74, 36 and 31 differential protein spots were found between OVC and OSCC, OVC and adjacent normal oral mucosa of OVC (OVCN), OSCC and adjacent normal oral mucosa of OSCC (OSCCN) samples, respectively. By identification of protein spots from 2-DE gels, 20 PMF maps were obtained by MALDI-TOF-MS including recoverin (cancer associated retinopathy (CAR) protein) tumor protein D53 (hD53), zinc finger protein 77 (ZNFpT1) and so on and these protein may play a key role in the carcinogenesis of OVC and OSCC.

Key words: Oral verrucous carcinoma, oral squamous cell carcinoma, two-dimensional electrophoresis, peptide mass fingerprints, matrix-assisted laser desorption/ionization-time of flight mass spectrometry.

INTRODUCTION

Oral verrucous carcinoma (OVC) is a rare variant of oral squamous cell carcinoma (OSCC) with a characteristic morphology and specific behaviors. The tumor occurs frequently in the oral cavity and larynx (Koch et al., 2001; McCoy and Waldron, 1981), representing anywhere from 1 to 10% of all oral squamous malignancies (Bouquot, 1998). The common sites of involvement in the mouth are the buccal mucosa and the gingiva, the alveolar ridge, the palate and the tongue. Comparing with conventional squamous cell carcinomas of the head and neck, they tend to present at an advanced age, with a higher proportion of male patients. It is a slow growing, low-grade, well-differentiated tumor that presents clinically as an exophytic, verrucoid papule or plaque on the skin or mucosa (Batsakis et al., 1982). Lymph node and distant metastases are rare during any stage of this tumor (McCoy and Waldron, 1981; Batsakis et al., 1982). However, they cause significant morbidity because of

*Corresponding author. E-mail: tangzhangui@yahoo.com.cn. Fax: +86-731-84805480.

Abbreviations: OVC, Oral verrucous carcinoma; **OSCC,** oral squamous cell carcinoma; **SDS,** sodium dodecyl sulphate; **TFA,** trifluoroacetic acid; **DTT,** dithiothreitol; **IPG,** immobiline pH-gradient; **PBS,** phosphate buffered saline; **DTE,** 1, 4-dithioerythritol; **NCBI,** National Center for Biotechnology Information; **CAR,** Cancer associated retinopathy; **IEF,** isoelectric focusing.

their local invasiveness and their pattern of stubborn recurrence with the currently acceptable modalities of radiation, surgery and intraarterial chemotherapy (Elliott et al., 1973; Krishnan et al., 1988; Wu et al., 2008).

In contrast to the traditional concepts, OVC is recently classified into three kinds of clinical phenotypes including exogenic type, infiltrative type and cystoid type. Lymph node and implant metastasis can be found in infiltrative type and cystoid type (Schrader et al., 1987; Tang et al., 2005). The mechanisms behind OVC's phenotypes remain unknown.

The study is able to identify the entire protein components' changes in the tissues which can provide insight into the mechanisms of the diseases and can help to discover biomarkers for diagnosis and guide clinic therapeutics (Banks et al., 2000; Graves and Haystead, 2002). In the present work, we applied proteomic analysis to identify the abnormal protein levels in OVC and OSCC patients.

MATERIALS AND METHODS

Patients and tissue sampling

Frozen samples from four patients with OVC and four patients with OSCC were obtained from Central South University Xiangya Hospital (Changsha, China). The pairs of underwent surgical specimens from both tumour and adjacent normal mucosa were collected. The age of the patients of OVC at the time of diagnosis are 38\35\53\46 (all are males) with a mean of 43 years, and OSCC are 63\53\68\60 (one female and the other are males) with a mean of 61 years. According to the criteria from the American Joint Committee on Cancer for pathological stages, there were 4 of T3N0 and 4 of T2N0. The stage of the cancer was defined by the extent of the lesion and was determined by physical examination, radiological studies and morphological examination. The histological diagnosis was made by two independent histopathologists. No tumor cells were detected in the surrounding mucosal tissues by histological examination. The study was approved by the ethical committee of Human Ethics Committee of Hunan Province, China.

Chemicals and materials

Tetramethylethylethylendeiame (TEMED) and acetonitrile were purchased from Sigma (St Louis, MO, USA). Urea, sodium dodecyl sulphate (SDS), glycine, Tris, bromophenol blue, ammonium persuphate, trypsin (sequencing grade), a-cyano-4-hydroxycinnamic acid (a-HCCA), trifluoroacetic acid (TFA), dithiothreitol (DTT), acrylamide, methylenebisacrylamide, CHAPS, thiourea and iodoacetamide were purchased from Shanghai Biocompany. PhastGel Blue tablets, immobiline pH-gradient (IPG) strip (pH 3 to 10), pharmalyte (pH 3 to 10), IPG buffer (pH 3 to 10) were obtained from Amershan Pharmcia, USA.

Protein preparation

All tissues were rinsed using phosphate buffered saline (PBS) and minced into pieces of about 1 to 2 mm^3 and then homogenized with 0.5 ml lysis buffer (8 mol/l urea, 4% CHAPS), containing protease inhibitor cocktail, by a homogenizer for 60 s at 6500 rpm. The lysates were centrifuged at 8000 rpm for 20 min at 4℃ and supernatants were collected for acetone precipitation for protein purification. The protein pellet was denatured with sample buffer (8 mol/l urea, 4% CHAPS, 65 mmol/l 1, 4-dithioerythritol (DTE), 0.5% ampholytes). The denatured proteins were incubated at 4℃ 2 to 3 h before centrifugation at 13,000 rpm for 15 min. The protein concentrations of the resulting supernatants were measured.

Two-dimensional difference gel electrophoresis

600 µg protein extractions per sample were taken for two dimensional (2D) gel separation. The extracted samples were diluted to 450 µl with rehydration buffer consisting of an 8 mol/l urea, 4% CHAPS, 65 mmol/l DTE, 0.5% ampholytes and traced by bromophenol blue. The rehydration solution was applied into immobilized pH gradient pH 3 to 10 IPG strip (240 mm× 3 mm× 0.5 mm) overnight. Electrophoresis in the first dimension was focused for a total of 64980 V h at 20℃ and then was as following 20℃ 30 V for 16 h (rehydration), 500 V for 1 h, grad 1000 V for 1 h, grad 3500 V for 2 h and 8000 V for 7.5 h. After isoelectric focusing (IEF), the strips were first equilibrated in equilibration solution of 50 mM Tris-HCl (pH 8.8), 6 M urea, 30% (V/V) glycerol, 2% (W/V) SDS and 1% (W/V) DTT for 15 min and later in the same solution except that DTT was replaced by 4% (W/V) iodoacetamide for another 15 min. Finally, the strip was transferred to the top of 12% polyacrylamide gels and held in position with molten 0.5% agarose in running buffer containing 25 mmol/l Tris, 0.192 mol/l glycine and 0.1% SDS. Gels were run at 20 mA/2 gels for 20 min followed by 40 mA/2 gel for 4 to 6 h.

Image and statistic analysis

Gels were routinely stained with silver nitrate and then scanned by 300 DPI imaging densitometer with image master 2D Elite software. Protein spots were quantified using the image master 2D elite software. To compare the tumor with normal samples from 8 patients, we screened the over-expressed proteins (≥5-fold) in tumor samples for the advance analysis. Comparisons were made between gel images of individual tumor and normal samples by image master 2D elite software. The pixel volume of each spot was calculated, normalized and compared between the two groups with t-test. Every gel was normalized with its internal standard image. Normalized volume differences were statistically calculated. Consistently and significantly over-expressed spots (≥5-fold) were averaged in each protein and selected for analysis.

Protein identification

Gel plugs picked were digested with trypsin automatically on Ettan Digester. First they were destained with 50 mM NH4HCO3 and 50% methanol and then dehydrated with 50% acetonitrile (ACN) and 0.1% trifluoroacetic acid (TFA). After the gel plugs were completely dried, trypsin solution (20 ng/ll in 20 mM ammonium bicarbonate) was added and the samples were digested at room temperature overnight. The extracted peptides were removed, dried and resuspended in 50% ACN-0.1% TFA. Equal volume of sample and a-HCCA were spotted and mixed on the MALDI-TOF target slides by Ettan spotter (Millipore, USA). Peptide extracts were analyzed on a MALDI-TOF-MS (BRUKERGS, USA) in positive ion reflectron mode. The accelerating potential was 20 KV with eight-shots per second. Trypsin auto digestion peaks were used as internal calibration and hACTH (19-39) and Ang III as external. Peptide mass data were searched against National Center for Biotechnology Information (NCBI) with the search engine of profound with homo sapiens as the species searched. The basic

requirement for identification was that the expectation value is <0.05 (<5% chance of error) and the coverage is >20%. The results were further confirmed in the Swissprot protein database (http://www.us.expasy.org/sprot).

RESULTS

Proteomic patterns of OVC and OSCC by 2-DE

Proteins obtained from tumour and adjacent normal tissues were separated by 2-DE. Spots were visualized with silver staining (Figures 1 and 2). Three pairs of gels from OVC and OSCC were analyzed using the image master 2D elite software. Nearly 1200 proteins spots were obtained in the range of Mr 14,400-9 4000 u, PI 3-10.

Averages of 1186 spots of OVC and 1076 spots of OSCC were detected across all gels. Fully automated spot detection and quantification were performed for paired samples by image master 2D elite software. The ratio values were compared and abundance ratios between different samples from different gels were calculated. The ratio values were expressed as fold changes. And a 5-fold increase in tumors was expressed as 5.0. In the OVC tissues, 36 commonly differential protein spots were found by comparing with the paired normal tissue. There were only 10 protein spots that consistently showed significant over-expression in all OVC tissues. Statistical analysis is summarized in Table 1, to indicate fold differences in OVC tissues, against the normal tissue pairs. Among the 10 over-expressed proteins, D53 was the lowest (5.13-fold). In the OSCC tissues, 31 commonly differential protein spots were found by comparing with the normal tissue pairs. There were 10 protein spots that consistently showed significant over-expression in all OSCC tissues. Statistical analysis were summarized in Table 2, to indicate fold differences in OSCC tissues, details and statistical analysis were summarized in Table 2.

Protein identification by MALDI-TOF MS analysis

Ten distinct protein spots were excised from gels randomly and marked with numbers at the corresponding sites in Figures 1 and 2. All spots obtained the PMF maps by MALDI-TOF MS following in-gel digestion with TPCK-trypsin. Figures 3 and 4 showed the spectrum of trypsin digestion of protein spot 6 in tumour tissue and protein spot 3 in the matching normal tissue. The results are summarized in Tables 3 and 4. Among those 10 over-expressed proteins, most of the matched proteins had high sequence coverage, accession number, theoretical Mr (kDa)/pI and MOWSE scores.

DISCUSSION

Oral squamous-cell carcinoma (SCC) is the most common cancer of the head and neck and accounts for over 300 000 new cancer cases worldwide annually (Lippman et al., 2005). Oral cancer remains one of the leading causes of death among human. As a rare variant of SCC, oral verrucous carcinoma (OVC) has a frequency of 0.3 to 10% occurred within the oral cavity (Bouquot, 1998; Kouzu et al., 2006). Recently, new protein markers have to be identified for its early detection and it is important in cancer early diagnosis and treatment. Using the 2-DE technology, picking out single spots, tryptic digestion and sequencing by MS to identify new potential biomarkers by proteomics is also a current and effective technology. The protein spots of interest could be been used to identify potential biomarkers for the disease. Our previous studies have indicated that, OVC has three kinds of clinical phenotypes and has a difference in genotypes compared with its matching normal tissue (Tang et al., 2007). To further understand the cellular function of OVC, we performed proteomics analysis to investigate the level of specific proteins related to OVC.

Ten of the total 1186 proteins with over 5.0-fold induction were consistently identified within 4 OVC cases by this proteomic analysis (Table 1). They may play a role in the malignant alteration of oral mucosal epithelial cells.

Cancer associated retinopathy (CAR) is paraneoplastic syndrome of ocular manifestation of paraneoplastic syndrome and is clinically characterized by progressive visual impairment which is similar to retinitis pigmentosa. The pathogenesis of CAR is assumed to be the result of retinal cell apoptosis with the expression of a photoreceptor protein (recoverin) through autoimmunity (Shiraga and Adams 2002). Recoverin is a calcium-binding protein that is expressed in retinal photoreceptors. It appears to delay the termination of the phototransduction cascade by blocking the phosphorrylation of photoexcited rhodopsin. Recoverin is expressed in one novel small cell lung carcinoma cell line (SCLC, KK0206), which is derived from a relapsed SCLC patient with CAR but without recoverin expression. The reason is that CAR patient with negative recoverin expression is unknown (Makoto et al., 2007). In our study, there is 22 fold difference for recoverin expression between OVC and its matching tissue, the function of recoverin in OVC development may need to be furthermore investigated in future.

The zinc finger gene (ZNF) family plays an important role in the regulation of transcription (Tarik et al., 2008). Members of this family are exclusively fungal and possess the well-conserved motif CysX2CysX6CysX5-12CysX2CysX6-8Cys (Sarah et al., 2006).The cysteine residues bind to two zinc atoms, which coordinate folding of the domain involved in DNA recognition. Since the discovery of Gal4p, many other zinc cluster proteins have been characterized; their function was in a wide range of processes, including primary and secondary metabolism and meiosis. Other roles include regulation of genes involved in the stress response as well as pleiotropic drug

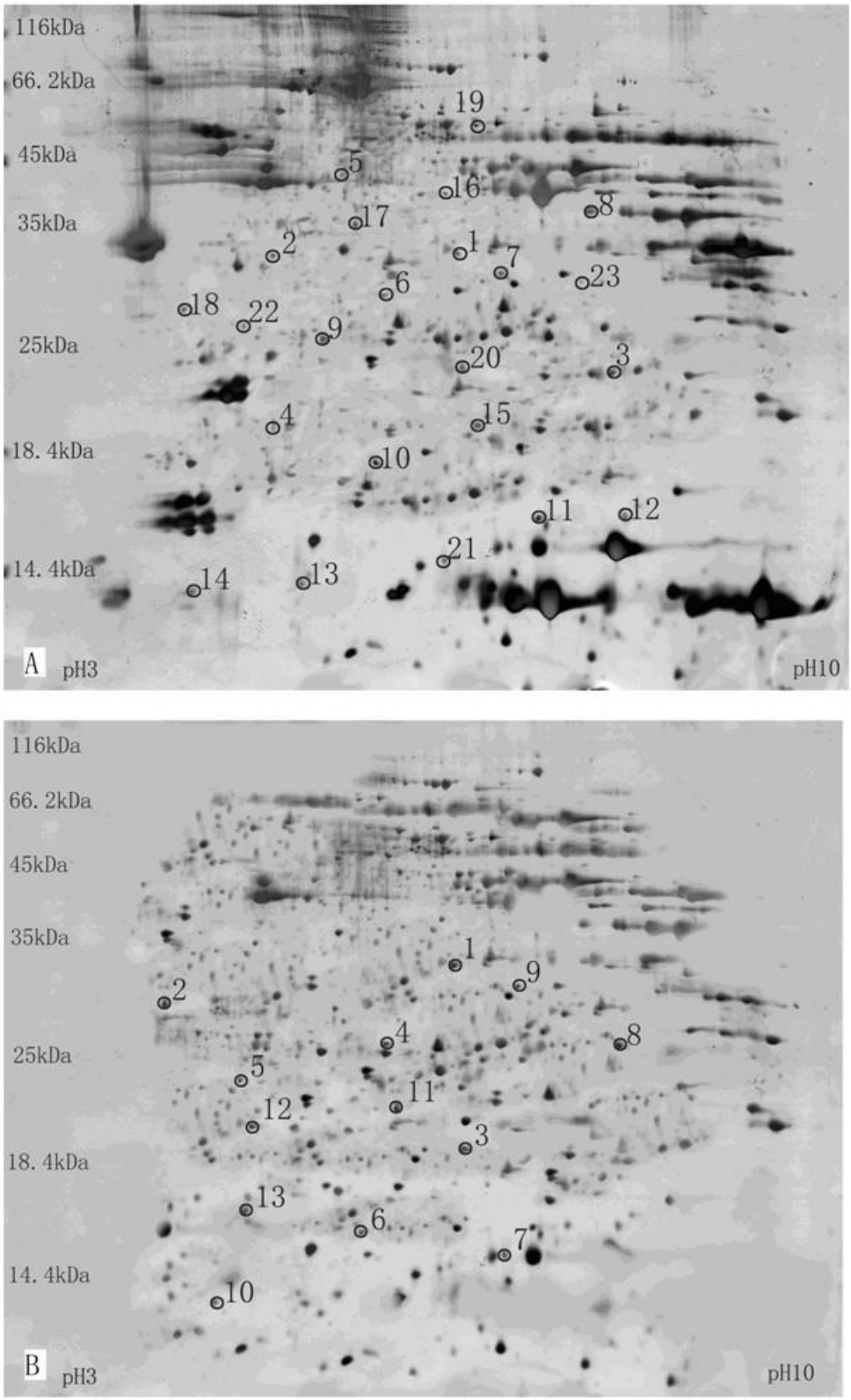

Figure 1. 2-DE map of human oral verrucous carcinoma tissue and the normal tissue pair extracts Six hundred micrograms of proteins were separated on 24 cm gels followed by silver staining. (A) Protein expression profiles of tumour tissue from one OVC patients; (B) the profiles of matched adjacent normal tissues from the same patients (the numbers means the commonly differential protein spots).

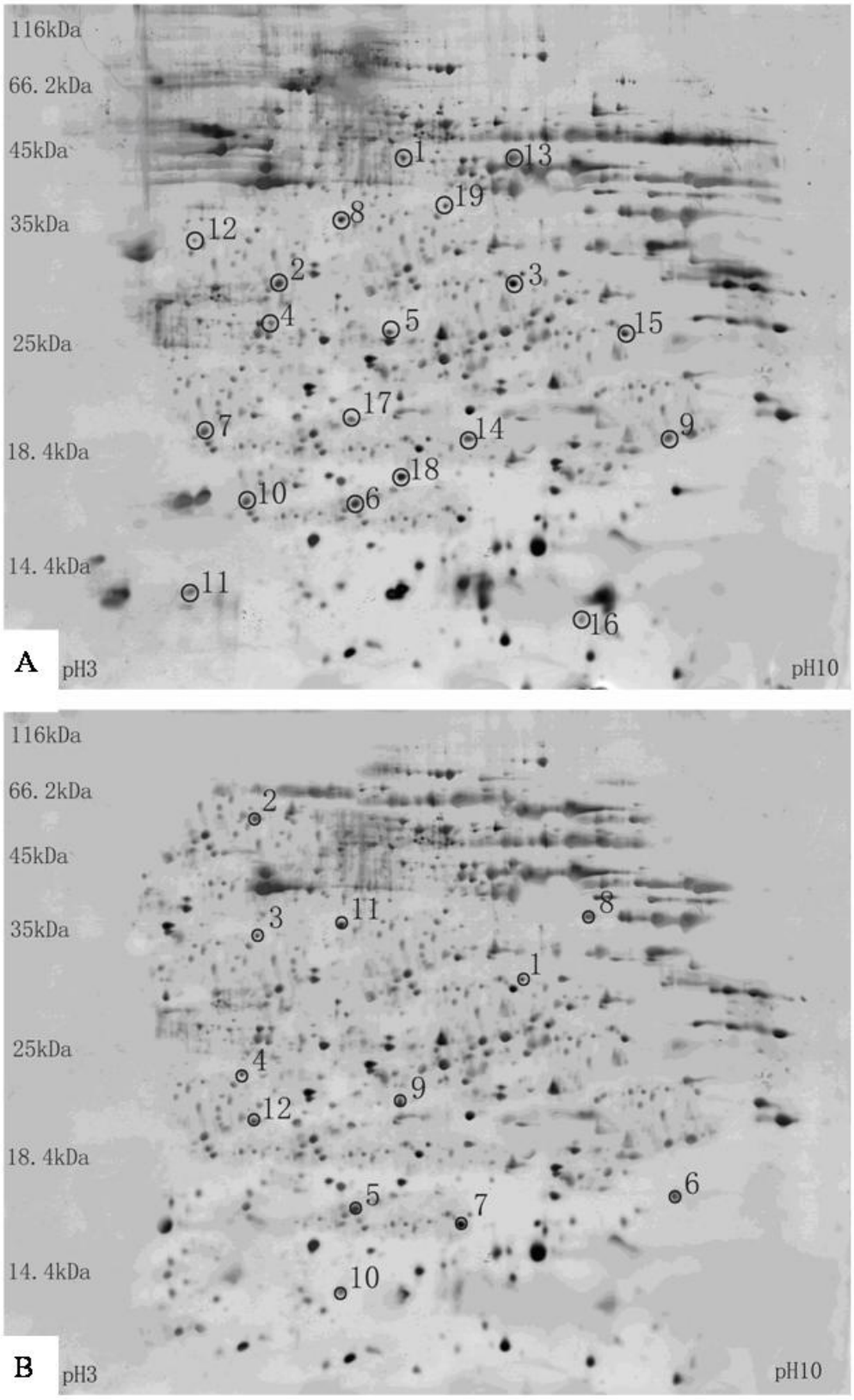

Figure 2. 2-DE map of human Oral squamous cell carcinoma tissue and the normal tissue pair extracts. Six hundred micrograms of proteins were separated on 24 cm gels followed by silver staining. (A) Protein expression profiles of tumour tissue from one OSCC patients; (B) the profiles of matched adjacent normal tissues from the same patients.

Table 1. Ten over-expressed proteins in OVC tissues comparing with adjacent normal tissues.

Spot no.	Protein ID	OVC (volume)	Normal tissue (volume)	Over-expression fold
V1	Tumor protein D53	70656±293	13773±326	5.13
V2	Recoverin (CAR protein)	92812±269	4161±103	22.30
V3	Ras-related protein Rap-2a	52820±373	7871±156	6.71
V4	S-phase kinase-associated protein 1A	22841±432	2367±97	9.65
V5	DNA repair protein RAD51 homolog 4	49139±398	5992±163	8.20
V6	Ras-related protein Rab-3B	32782±261	4629±172	7.08
V7	Zinc finger protein 77	40220±308	3901±125	10.31
N1	Isoform of Nuclear receptor ROR-alpha	7502±141	49439±157	6.59
N2	Modulator recognition factor protein 2	6956±291	55928±263	8.04
N3	Vitamin K-dependent protein C light	3620±194	18968±443	5.24

Table 2. Ten over-expressed proteins in OSCC tissues comparing with adjacent normal tissues.

Spots no.	Protein ID	OVC (volume)	Normal tissue (volume)	Over-expression fold
T1	Phospholipase A2 inhibitory protein	51468±652	8889±348	5.79
T2	Melanoma antigen recognized by T-cells 1(MART-1)	38879±421	4438±291	8.76
T3	Isoform of DNA-binding protein Ikaros	48283±186	7568±237	6.38
T4	CHAIN 1: Endothelial cell-specific molecule 1	18397±339	3426±265	5.37
T5	Isoform of caspase-6 precursor (EC 3.4.22)	22906±145	4527±210	5.06
T6	CHAIN 2:Complement factor I heavy chain	64583±384	8704±163	7.42
T7	Eukaryotic translation initiation factor 2 subunit 2(Eukaryotic translation initiation factor 2 beta subunit)	24346±525	4517±265	5.39
N1	Calbindin (Vitamin D-dependent calcium-binding protein, avian-type)	12975±360	76814±605	5.92
N2	Zinc-finger protein ubi-d4(Requiem) (Apoptosis response zinc finger protein)	13495±293	85562±347	6.34
N3	Isoform of Nuclear receptor ROR-alpha (Nuclear receptor RZR-alpha)	8128±265	58203±298	7.16

resistance, as demonstrated in budding yeast and in human fungal pathogens. With the number of characterized zinc cluster proteins growing rapidly, it is becoming more and more important (Li et al., 2008; Li et al., 2007; Huang et al., 2007).

The putative adaptor protein D53, a member of the D52-like family, works as a novel 14-3-3 binding partner in breast cancer cells9 (Boutros et al., 2003). Recently, studies show that cytoplasmic protein whose capacity to bind 14-3-3 is regulated by the alternative splicing of an exon encoding a canonical 14-3-3 binding motif (Boutros et al., 2003). D52-like proteins were first identified for their expression in breast cancer (Mona et al., 2008; Wang et al., 2004; Nourse et al., 1998) and confirmed with numerous studies for D52 upregulation in human breast (Balleine et al., 2000; Pollack et al., 2002; Ross and Perou, 2001) and other (Cao et al., 2006; Rhodes et al., 2002) cancers. Recent microarray studies have identified D53 as a gene whose transcript abundance significantly varies according to cell cycle stage in primary human fibroblasts (Cho et al., 2001) and HeLa cells (Whitfield et al., 2002; Wichert et al., 2004) or according to circadian rhythms in mouse liver (Wei et al., 2006). In the latter study, D53 was reported to form part of gene cluster implicated in cell division, cell death and chromosome segregation (Akhtar et al., 2002). This study found that, D53 was highly over expressed in tumour than its matched normal indicating that it may be used as a differentiation marker.

In conclusion, we identified 10 proteins just as recoverin (cancer associated retinopathy protein), (CAR protein) tumor protein D53 (hD53), zinc finger protein 77 (ZNFpT1) may be involved in the pathogenesis of OVC and they may be used as potential markers for the

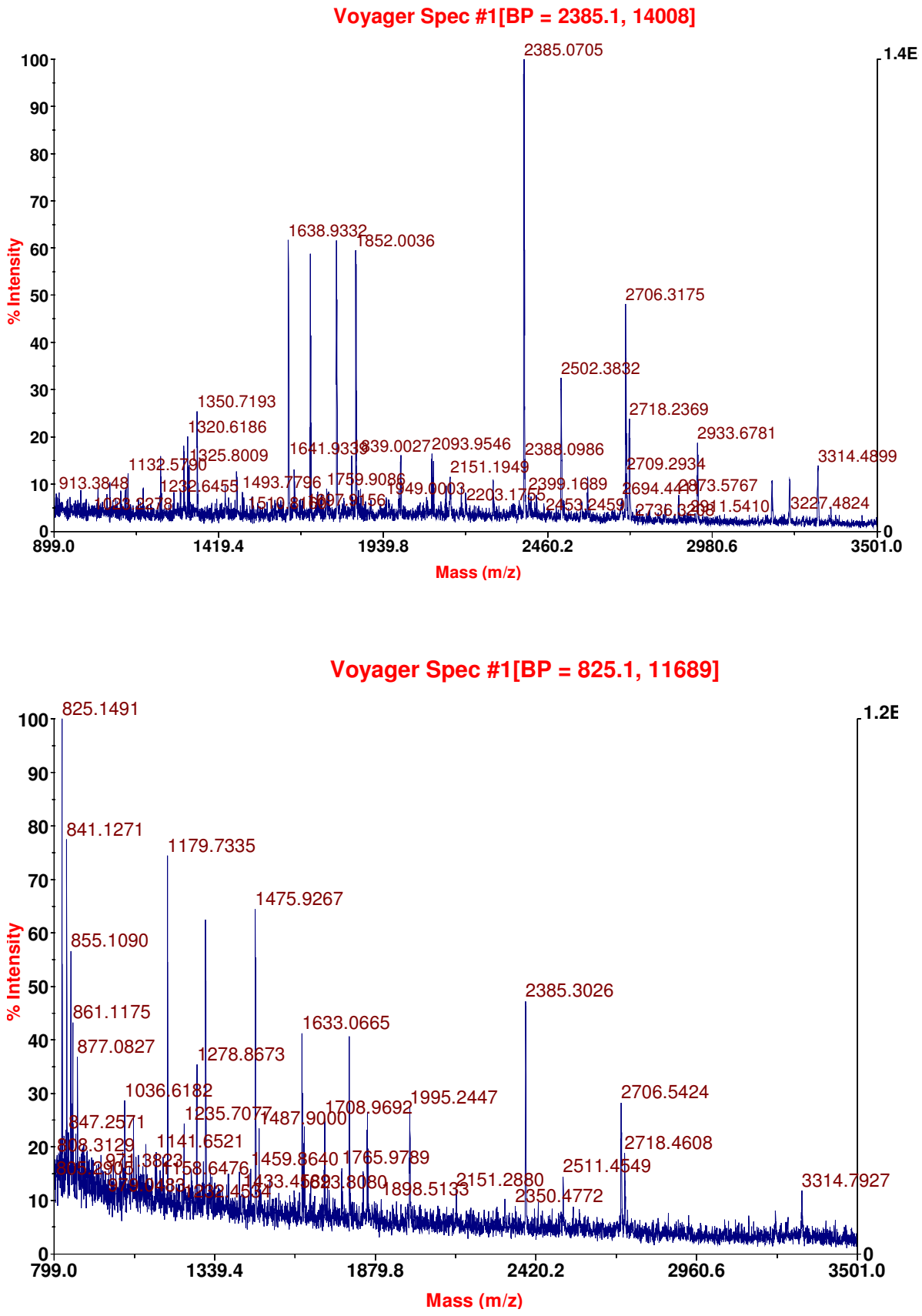

Figure 3. PMF of protein spot 3 and spot 6 in OVC 2-DE map (N3 upper and V6 down).

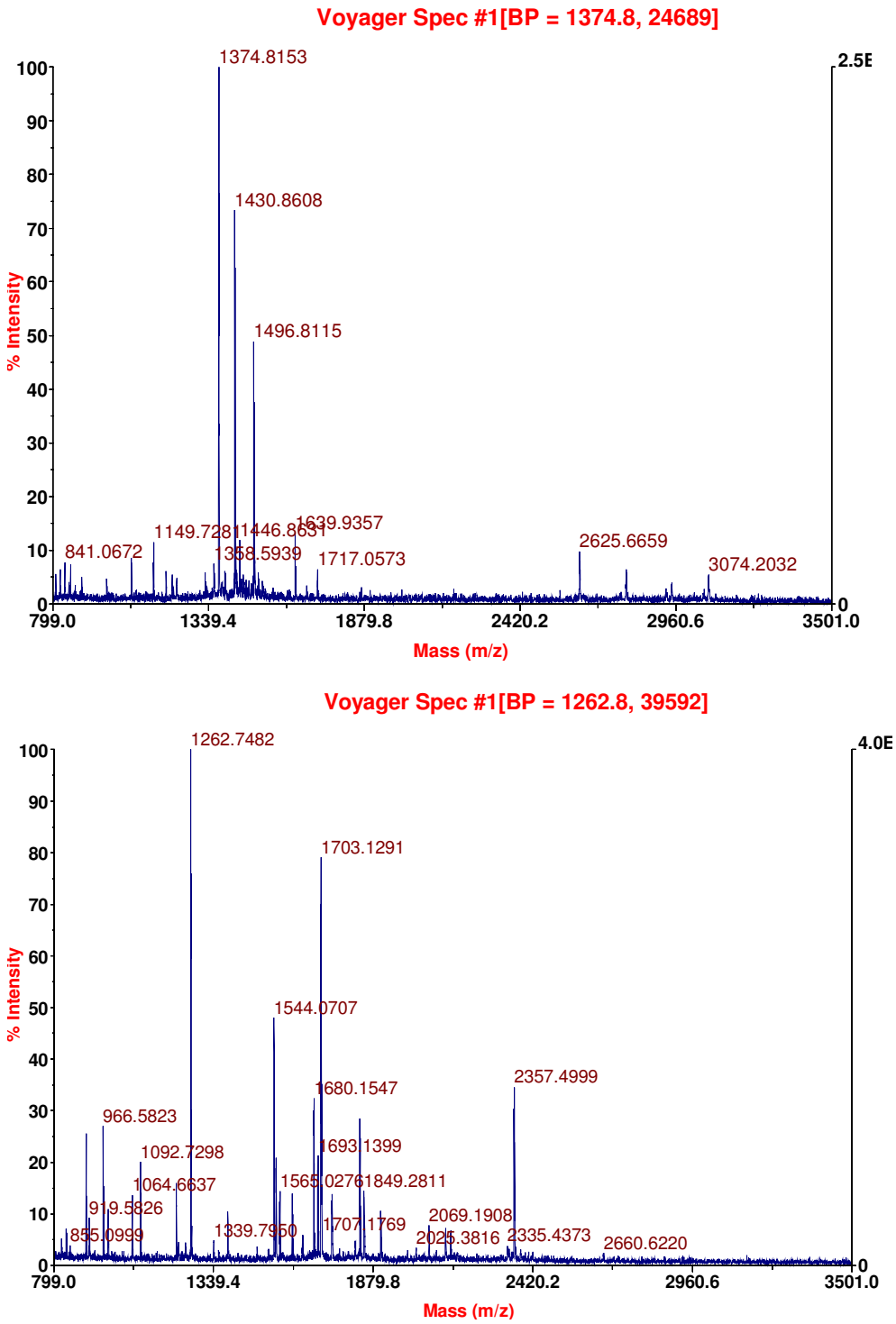

Figure 4. PMF of protein spot 3 and spot 6 in OSCC 2-DE map (N3 upper and T6 down).

diagnosis and prognosis.

ACKNOWLEGDEMENTS

This project was supported by The National Natural Science Foundation of China (30872895), the key Program of Department of Science and Technology of Hunan (2008FJ2011) and the Science Foundation for Post-doctoral Scientists of Hunan, China (Grant No.2006FJ4246). We thank Dr. Shan Gao for his critical

Table 3. Protein spots in OVC tissue and the matched normal tissue searched by peptident software in database.

Spot no.	#Peptide matches	AC	Description	pI	Mass weight	Coverage%
V1	4/21	Q16890	Tumor protein D53 (hD53) (D52-like 1). - Homo sapiens (Human).	5.45	22449.07	24.5
V2	4/26	P35243	Recoverin (Cancer associated retinopathy protein) (CAR protein). - Homo sapiens (Human)..	5.06	22999.07	31.7
V3	4/25	P10114	Ras-related protein Rap-2a. - Homo sapiens (Human).	4.73	20615.46	31.1
V4	6/32	P34991	S-phase kinase-associated protein 1A (Cyclin A/CDK2-associated protein p19) (p19A) (p19skp1) (RNA polymerase II elongation factor-like protein).	4.40	18526.81	22.2
V5	5/33	075771	DNA repair protein RAD51 homolog 4 (R51H3) (TRAD). - Homo sapiens (Human).	5.89	35049.32	18.0
V6	4/22	P20337	Ras-related protein Rab-3B. - Homo sapiens (Human).	4.85	24757.90	19.6
V7	5/17	Q15935	Zinc finger protein 77 (ZNFpT1) (Fragment). - Homo sapiens (Human).	undefined	undefined	33.9
N1	4/13	Q96E17	Isoform of Nuclear receptor ROR-alpha (Nuclear receptor RZR-alpha) - Homo sapiens (Human).	5.09	25952.19	16.3
N2	4/29	Q14865	Modulator recognition factor protein 2 (Mrf-2) - Homo sapiens (Human)..	undefined	undefined	16.5
N3	5/26	P04070	CHAIN 2: Vitamin K-dependent protein C light - Homo sapiens (Human).	5.33	17583.91	16.1

Table 4. Protein spots in OSCC tissue and the matching normal tissue searched by peptident software in database.

Spot no.	#Peptide matches	AC	Description	pI	Mass weight	Coverage (%)
T1	19/29	P04083	Phospholipase A2 inhibitory protein	6.54	38583.05	64.3
T2	4/17	Q16655	Melanoma antigen recognized by T-cells 1(MART-1) (Melan-A protein) (Antigen SK29-AA) (Antigen LB39-AA) Homo sapiens (Human).	5.29	23157.03	22.9
T3	6/22	Q13422 (Isoform)	Isoform of DNA-binding protein Ikaros (Lymphoid transcription factor LyF-1).- Homo sapiens(Human).	5.75	47633.96	18.7
T4	7/22	Q9NQ30	CHAIN 1: Endothelial cell-specific molecule 1.- Homo sapiens(Human).	5.83	28122.42	50.3
T5	4/23	P55212 (Isoform)	Isoform of Caspase-6 precursor (EC 3.4.22.-) (Apoptotic protease Mch-2).- Homo sapiens (Human).	6.69	22573.80	21.5
T6	6/25	P05156	CHAIN 2: Complement factor i heavy chain - Homo sapiens (Human).	5.69	25286.22	24.9
T7	4/19	P20042	Eukaryotic translation initiation factor 2 subunit 2(Eukaryotic translation initiation factor 2 beta subunit) (eIF-2-beta) - Homo sapiens (Human).	5.60	28388.41	15.0
N1	5/25	P05937	Calbindin (Vitamin D-dependent calcium-binding protein, avian-type) (CalbindinD28) (D-28K) - Homo sapiens (Human).	4.70	29893.91	25.4
N2	5/20	Q92785	Zinc-finger protein ubi-d4 (Requiem) (Apoptosis response zinc finger protein) - Homo sapiens (Human).	5.94	44155.48	18.4
N3	7/25	P35398 (Isoform)	Isoform of Nuclear receptor ROR-alpha (Nuclear receptor RZR-alpha) - Homo sapiens (Human).	5.14	53598.32	21.4

reading of the manuscript.

REFERENCES

Akhtar RA, Reddy AB, Maywood ES, Clayton JD, King VM, Smith AG, Gant TW, Hastings MH, Kyriacou CP (2002). Circadian cycling of the mouse liver transcriptome, as revealed by cDNA microarray, is driven by the suprachiasmatic nucleus. Curr. Biol. 12: 540-550.

Balleine RL, Fejzo MS, Sathasivam P, Basset P, Clarke CL, Byrne JA (2000). The hD52 (TPD52) gene is a candidate target gene for events resulting in increased 8q21 copy number in human breast carcinoma. Genes, Chromosomes Cancer, 29: 48-57.

Banks RE, Dunn MJ, Hochstrasser DF, Sanchez JC, Blackstock W, Pappin DJ, Selby PJ (2000). Proteomics: new perspectives, new biomed. opportunities. Lancet, 356: 1749-1756.

Batsakis JG, Hybels R, Crissman JD, Rice DH (1982). The pathology of head and neck tumors: verrucous carcinoma. Part15, Head Neck Surg. 5: 29-38.

Boutros R, Bailey AM, Wilson SH, Byrne JA (2003). Alternative splicing as a mechanism for regulating 14-3-3 binding: interactions between hD53 (TPD52L1) and 14-3-3 proteins. J. Mol. Biol. 332: 675-687.

Bouquot JE (1998). Oral verrucous carcinoma: incidence in two US populations. Oral Surg Oral Med Oral Pathol. Oral. Radiol. Endod. 86: 318-24.

Cao Q, Chen J, Zhu L (2006). A testis-specific and testis developmentally regulated tumor protein D52 (TPD52)-like protein TPD52L3/hD55 interacts with TPD52 family proteins. Biochem. Biophys. Res. Commun. 344: 798-806.

Cho RJ, Huang M, Campbell MJ, Dong H, Steinmetz L, Sapinoso L, Hampton G, Elledge SJ, Davis RW, Lockhart DJ (2001). Transcriptional regulation and function during the human cell cycle. Nat. Genet. 27: 48-54..

Elliott GB, MacDougall JA, Elliott JDA (1973). Problems of verrucous squamous carcinoma. Ann. Surg. 17: 309-314.

Graves PR, Haystead TA (2002). Molecular biologist's guide to proteomics. Microbiol. Mol. Biol. Rev. 66: 39-63

Huang C, Jia Y, Yang S (2007). Characterization of ZNF23, a KRAB2 containing protein that is downregulated in human cancers and inhibits cell cycle progression. Exp. Cell Res. 313(2): 254-263.

Krishnan Nair M, Sankaranarayanan R, Padmanabhan TK (1988). Oral verrucous carcinoma: treatment with radiotherapy. Cancer, 61: 458-61.

Koch BB, Trask DK, Hoffman HT, Karnell LH, Robinson RA, Zhen W, Menck HR (2001). National survey of head and neck verrucous carcinoma. Cancer, 92: 110-120.

Kouzu Y, Uzawa K, Koike H, Saito K, Nakashima D, Higo M, Endo Y, Kasamatsu A, Shiiba M, Bukawa H, Yokoe H, Tanzawa H (2006). Overexpression of stathmin in oral squamous-cell carcinoma: correlation with tumour progression and poor prognosis. Br. J. Cancer, 94(5): 717-723.

Lippman SM, Sudbo J, Hong WK (2005). Oral cancer prevention and the evolution of molecular-targeted drug development. J. Clin. Oncol. 23: 346-356.

Li Y, Yang D, Bai Y (2008). ZNF418, a novel human KRAB/C2H2 zinc finger protein, suppresses MAPK signaling pathway. Mol. Cell Biochem. 310(1-2): 141-151.

Li J, Wang Y, Fan X (2007). ZNF307, a novel zinc finger gene suppresses p53 and p21 pathway. Biochem Biophys Res. Commun. 363(4): 895-900.

McCoy JM, Waldron CA (1981). Verrucous carcinoma of the oral cavity. A review of forty-nine cases. Oral Surg Oral Med Oral Pathol. Oral Radiol. Endod. 52: 623-629.

Makoto K, Takayuki I, Yoshiki U, Tamotsu T, Hisayuki U, Yuji O, Hirokuni T (2007). Establishment of a novel small cell lung carcinoma cell line with specific recoverin expression from a patient with cancer-associated retinopathy. Lung Cancer, 56: 319-326.

Mona S, Ivan B, Rose B, Judith W, Susan F, Lisa S, Nikolajs Z, Karen B, Robert KB, Rosette L, Jennifer AB (2008). Nonredundant Functions for Tumor Protein D52-Like Proteins Support Specific Targeting of TPD52.Clin. Cancer Res., 14: 5050-5060.

Nourse CR, Mattei MG, Gunning P, Byrne JA (1998). Cloning of a third member of the D52 gene family indicates alternative coding sequence usage in D52-like transcripts. Biochim. Biophys. Acta. 1443: 155-168.

Pollack JR, Sorlie T, Perou CM, Rees CA, Jeffrey SS, Lonning PE, Tibshirani R, Botstein D, Borresen-Dale AL, Brown PO (2002). Microarray analysis reveals a major direct role of DNA copy number alteration in the transcriptional program of human breast tumors. Proc. Natl. Acad. Sci. USA, 99: 12963-12968.

Ross DT, Perou CM (2001). A comparison of gene expression signatures from breast tumors and breast tissue derived cell lines. Dis. Markers. 17:99-109.

Rhodes DR, Barrette TR, Rubin MA, Ghosh D, Chinnaiyan AM (2002). Meta-analysis of microarrays: interstudy validation of gene expression profiles reveals pathway dysregulation in prostate cancer. Cancer Res. 62:4427-4433.

Shiraga S, Adams G (2002). Mechanism of CAR syndrome: antirecoverin antibodies are inducer of retinal cell apoptotic death via the caspase 9-and caspase 3-dependent pathway. J. Neuroimmunol.132:72-82.

Sarah MacPherson, Marc Larochelle, Bernard Turcotte (2006). A Fungal Family of Transcriptional Regulators: the Zinc Cluster Proteins. Microbiol. Mol. Biol. Rev., 70: 583-604

Schrader M, Laberke HG, Jahnke K(1987). Lymphatic metastases of verrucous carcinoma (Ackerman tumor). HNO, 35: 27-30.

Tang ZG, Xie XL, Li JY, Liu XC, Yao ZG, Zhao SP (2005). A clinic study on oral verrucous carcinoma phenotypes. Chin J. Den Res. 8(3): 57-61.

Tang ZG, Zhao SP, Zhang L, Li XL (2007). Gene expression profile changes in oral verrucous carcinoma and squamous cell carcinoma. Zhonghua Kou Qiang, Yi Xue, Za Zhi. 42(4): 229-230.

Tarik M, Hui Z, Jianmin J, Kurt WS (2008). Alexander Carpinteiro, Erich Gulbins. The zinc finger protein and transcriptional repressor Gfi1 as a regulator of the innate immune response. Immunobiology, 213: 341-352.

Wang R, Xu J, Saramäki O (2004). A novel prostate-specific and androgen-responsive gene of the TPD52 family, amplified in chromosome 8q21.1 and overexpressed in human prostate cancer. Cancer Res. 64: 1589-1594.

Wei LR, Xu JC, Li XB, Qian Q, Zhu LH (2006). Genetic Analysis and Mapping of the Dominant Dwarfing Gene *D-53* in Rice. J. Integrative Plant Biol. 48: 447-452.

Whitfield ML, Sherlock G, Saldanha AJ, Murray JI, Ball CA, Alexander KE, Matese JC, Perou CM, Hurt MM, Brown PO, Botstein D (2002). Identification of genes periodically expressed in the human cell cycle and their expression in tumors. Mol. Biol. Cell. 13: 1977-2000.

Wichert S, Fokianos K, Strimmer K (2004). Identifying periodically expressed transcripts in microarray time series data. Bioinformatics, 20: 5-20.

Wu CF, Chen CM, Shen YS, Huang IY, Chen CH, Chen CY,Shieh TY, Sheen MC(2008).EVective eradication of oral verrucous carcinoma with continuous intraarterial infusion chemotherapy. Head Neck, 30: 611-617.